Proceedings World Geothermal Congress 2000
Kyushu - Tohoku, Japan, May 28 - June 10, 2000

DEVELOPMENT OF HIGH TEMPERATURE DOWNHOLEMOTORS FOR GEOTHERMAL WELL DRILLING

Tsuguhiko Watanabe[1], Hikaru Kamiirisa[1], Teruo Masumoto[2] and Yoshio Yamada[2]
[1]Akishima Laboratories (Mitsui Zosen) inc., 1-50, Tsutsujigaoka 1-chome Akishima, Tokyo Japan
[2]YBM inc., 1534, Haru, Karatsu , Saga Japan

Key Words : downholemotor, positive displacement motor, elastomer, trochoidal curves, manufacturing, performance test

ABSTRACT

A high temperature downholemotor has been developed in a project sponsored by NEDO (New Energy and Industrial Technology Development Organization in Japan). We studied about three technical matters to achieve this development, and carried out the performance test with a scaled model of the downholemotor.
Under high temperature conditions, many kinds of elastomers were tested, in order to find out a suitable one for the stator. Compression tests for elastic recovery, abrasion tests between the rotor and the stator, and measurement of thermal expansion were carried out for each elastomer. The most suitable materials for the stator have been found now.
The downholemotor is a helicoidal type. In their cross sections, the rotor and the stator are designed with trochoidal curves, on which they gear into each other. These trochoidal curves, which are created as the off-set of the cycloid curve, improve endurance performance and provide a sealing function between a rotor and a stator even in a high temperature environment.
Both the rotor and the stator, designed with these curves, are manufactured by a numerical controlled machining center, whose positional accuracy is within 0.05 millimeters. So they fit into each other smoothly and so high endurance performances are realized.
The scaled models of this high temperature downholemotor were fabricated for the performance test. Its outer diameter is 190.00 millimeters(almost 6-3/4 in) and its length is about 600 millimeters(1.95 ft) down to the full-scaled downholemotor, which is 171.5 millimeters (6-3/4 in) in its outer diameter and 6,000 to 8,000 millimeters (20 to 26.5 ft) in length. This performance test shows that its rotation is from 0 to 60 rpm and its torque is about 250 N-m (185 ft-lbf) maximum under 200 degree Celsius. We confirmed that the downholemotor can operate continuously over 30 hours under any temperature condition. These performances are nearly the same as those of downholemotors on the market restricted to normal temperature use.

1. DOWNHOLEMOTORS MOTOR SECTION

There are two types of downholemotors. One is a turbine type, and the other is a helicoidal type. The latter one is usually utilized in geothermal drilling fields, because it is appropriate for slow rotation and large torque, and its endurance is predictable. The downholemotor is composed with a shock-absorber section, a joint section, a by-pass section and a motor section (the motor assembly). Especially, the helicoidal downholemotor has a motor section, which converts mud flow in drill pipes to rotational power for the drilling bit. But its performance deteriorates in high temperature conditions, such as geothermal well drilling fields.
The motor section can be damaged fatally in such conditions when it is a conventional downholemotor. The rotor and the stator are the most important parts in this motor section, and the stator is conventionally made from natural rubber, which has poor performance under high temperature conditions.
The present study showed us a way to enhance the performance of the motor section, to apply some elastomer for high temperature and also development of a way to design and manufacture the motor section.

1.1 Elastomer for high temperatures

Under a high temperature condition (over 150 degree Celsius), the stators composed with the nitrile-butadiene rubber caused some troubles, such as the destruction at parts of the stator touching the rotor, the ablation at parts of the stator fitted with drill collar. These stators are ones of the conventional downholemotor.
Some kinds of elastomer, metal materials and ceramics for use in high temperatures were investigated to find out suitable ones as the stator material, and a method were developed to evaluate elastic recovery, thermal expansion, abrasion. These parameters made the seal function of each material to be cleared. The formula is as follows;

$$S = E + T - A - C \qquad (1)$$

S : Seal capacity
E : Elastic recovery
T : Thermal expansion
A : Abrasion
C : Clearance between the rotor and the stator

Elastic recovery was measured at a dynamic elastic-viscosity test. The experimental equipment for it is shown as Fig.1. Each sample for high temperature was heated up to 250 degree Celsius by a band-typed heater set around it, and compressed 4 kN (400 kgf) on the top side of it repeatedly over 6000 times. Stress σ and strain ε were measured during this test, and elastic recovery at any temperature could be known by the results of this experiment. Fig.2 is one elastic recovery of a tested elastomer.
Thermal expansions were measured as Fig.4. The expansion is nearly proportional to the temperature.
Abrasion tests were carried out by a apparatus shown as Fig.5. The ge-rotor in this equipment also has a rotor and a stator. This rotor moves around an eccentric center, as well as the motor section of downholemotors. So the abrasion on these stator samples can be simulated with this equipment. The water temperature in this tank goes up to 250 degree Celsius. This tank has the capacity for 4 MPa, for the water not to be vaporized. The rotor moves 320 turns in a minute. Evaluation of the abrasion can be done by PV(Pressure-Velosity) value. Each test was run for 30 hours to evaluate the endurance performance of each sample. The results of this test is shown

as Fig.6.
Clearance between the rotor and the stator was decided by the cross section design in the motor section.

1.2 The cross section design in the motor section

In the motor section of the conventional positive displacement motor (PDM), which is one kind of downholemotor, the rotor and the stator are manufactured with an arc-shaped curve. It is thought as one reason that endurance under high temperature conditions is very poor, so the rotor is sometimes stuck to the stator. To move the rotor smoothly around the stator and to extend the endurance of this motor section, the trochoidal curves were applied to the cross section design.
The trochoidal curves were created as a off-set of the cycloid curve. The motion of the rotor and the stator had no slides, so the abrasion was decreased. These curves are decided by some parameters, such as the number of robes, the eccentricity and the diameter of the base circles of the rotor and the stator. The relations between these parameters and the specification of downholemotors were studied, and some equations about them were determined out. Now the result of this study is judged as a patent.
Clearance between the rotor and the stator was designed when minimum and maximum diameters had been decided, according to the parameters about the material utilized for stators, such as elastic recovery, thermal expansion and abrasion.
The section design based on these study is drawn as Fig.7.

1.3 Manufacturing of the rotor and the stator

A part of a full scaled motor assembly was experimentally manufactured to meet the development specification. For the bonding between the stator and the outer tube, a key-way design was adopted and the trial manufacture was proved free from any specific problem.
The numerical controlled machining centers were used for manufacturing the rotor and the stator. They are shown as Fig.8, the maneuverable position of which can be controlled with a 0.001 millimeters order so that the manufactured rotors and stators are produced within 0.01 millimeters error. But 0.1 to 0.5 millimeters error can occur when the manufactured materials are changed. We had to adjust the setting of the ball-end-mill or the numerical control data, according to the manufactured materials. Table.1 shows the designed parameters for them. The new angle head is especially prepared for inner cutting to manufacture the stator, of which the length is about 300 millimeters maximum.
So that, the real downholemotor, which has a length of about 7000 millimeters, needs twenty-four stators. Every stator and the outer tube are sealed from each other by O-rings to prohibit the leak of drilling mud, to convert the mud flow to motor drive energy efficiently.

2. PERFORMANCE TESTS

2.1 Experimental apparatus

In order to evaluate the performance of the manufactured downholemotor, the experimental apparatus was constructed as Fig.9. It was designed for the simulation of the drilling system in actual geothermal well fields.
The system arrangement is shown as Fig.10. The water jet pump, with three plungers, regulates the flow rate in this circulation system, in maximum 800 litters per minutes. The electric magnetic brake gives the load of this scaled downholemotor. Two heater sets on the side of the scaled downholemotor and in the mud tank regulate the temperature in the test situation, up to 200 degree Celsius.

2.2 Efficiency

Flow rate Q of circulation is measured by a electric-magnetic flow meter. Pressure ΔP is measured at a pressure transducer at the upper side of the downholemotor. The rotation N of the rotor is measured by a optical revolution counter. Torque T generated by this downholemotor is measured by the torque converter at the horizontal shaft.
The total efficiency, the volumetric efficiency, and the mechanical efficiency are calculated by these parameters, Q, ΔP, N and T as follows;

$$\eta_t = \frac{2\pi NT/60}{\Delta PQ/60} \tag{2}$$

$$\eta_v = \frac{N \cdot q}{Q} \tag{3}$$

$$\eta_m = \frac{2\pi T}{\Delta P \cdot q} \tag{4}$$

η_t : Total efficiency
η_v : Volumetric efficiency
η_m : Mechanical efficiency
N : Rotational speed
T : Torque
ΔP : Differential pressure
Q : Flow rate
q : cell quantity (volume between the rotor and the stator)

2.3 Methods

Four sets of the rotor and the stator, which have been manufactured experimentally, were prepared for the performance tests. One set of rotors and stators are shown as Fig.11.
Three sets were used for the water circulation tests. One set was used for the room temperature test, another set for the 150 degree Celsius test, and the other for the 200 degree Celsius test. Every set was tested during all the endurable time, accumulated over 30 hours, which is one of the development specification. At the beginning of the test and at the time of 5, 10, and 30 hours past, the parameters, Q, ΔP, N and T were measured to estimate the dynamic performance of the downholemotor. And the rotor and the stator were decomposed immediately, and their minimum diameter, maximum diameter were measured and they were weighed to measure their endurance capability.
One set was used for the oil circulation test. Oil circulation tests were carried out to investigate the effect of the drilling mud viscosity.

2.4 Water circulation tests

The total efficiency, the volumetric efficiency and the mechanical efficiency were calculated by parameters, Q, ΔP, N and T, measured at each stage of the tests. The performance curves were drawn as Fig.12. The efficiency curves are drawn as Fig.13.
According to these performance curves, the relations between pressure ΔP and torque T, and between flow rate Q and rotational speed N, were found out. These relations are seen to all performance curves.

$$\Delta P \propto T \tag{5}$$

$$N \propto Q \tag{6}$$

In these tests, the performance of endurance was also estimated.
All the parameters for motor drive, such as Q, ΔP, N and T and the temperature of the fluid (water or oil) running through this experimental apparatus, were measured during all test. We can simulate this test condition as one of the well drilling fields.
The minimum diameter, the maximum diameter, and the weight of the rotor and the stator were measured at each time. In all test conditions, their diameters and their weight did not change so much. The endurance performance was proved by these data.
The performance curves at the beginning of the test and at the end (30 hours) of the test are comparable with Fig.12 and Fig.14. The efficiency curves are comparable with Fig.13 and Fig.15. The endurance performance was also proved by no difference can be seen between the beginning curve and the last curve.

2.5 Oil circulation tests

As well as water circulation tests, the performance curves of oil circulation tests were shown in Fig.16 and the efficiency curves were shown as Fig.17. There is one assumption that the volumetric efficiency is 100% when the motor section doesn't generate any torque without any loads, which is sure to be reasonable according to the volumetric efficiency curves in water circulation tests as Fig.13 and Fig.15.
Because the plunger pump was the jet pump designed for water, the flow rate was not enough to carry out oil circulation as effectively as water circulation tests. So data, measured as torque and rotational speed, were smaller in the oil circulation tests than in the water circulation tests. The higher viscosity of oil makes the efficiency (η_t, η_v, η_m) better than the water circulation tests, because it decreases the leak between the rotor and the stator.

2.6 Considerations

The performances with the usual mud flow can be understood by the result of the water circulation tests and the oil circulation tests. The viscosity of water, the oil utilized in these tests, and the typical drilling mud in usual drilling fields were compared on the Table2. This table shows that the viscosity of oil is 7.01×10^{-3} Pa･s and the viscosity of oil is 7 to 12.5×10^{-3} Pa･s under the temperature 150 degree Celsius, so the performance with drilling mud are supposed to be similar to the oil circulation tests.
The volumetric efficiencies increase when the temperature of the circulation water goes higher. It is thought that the thermal expansion and the elastic function solidifies the contact between the rotor and the stator and improves the seal function.
The measured torque is proportional to the pressure given by the pump. The trend at each flow rate is same. Based upon the formula (4) about η_m, we can think that the mechanical efficiency is monotonously increased and it shall approach the ratio of torque and pressure.
The total efficiency curve tells us the best flow rate for each torque when we need to drill the wells by downholemotors.

3. CONCLUSIONS

Through these studies, a method of manufacturing downholemotors has been assured to be realized in our Japanese industries. Especially it is remarkable that downholemotors for high temperature conditions has been developed.
Some elastomers has been elected as suitable materials for the stator of downholemotors for geothermal well drilling, however conventional ones made from nitrile-butadiene rubber do not perform endurance enough.
The motor section designed with trochoidal curves has been assured to have good performance of endurance under high temperature conditions.
The accumulated composition of stators has been assured to manufacture the real downholemotors.
A part of a full scaled model has been manufactured and experimented in the performance tests. We succeeded to study the trend and characteristic functions of prototyped models, and they were similar to one of the conventional downholemotor.

4. ACKNOWLEDGEMENTS

This study was supported not only on the economical management but also on the technical matter by NEDO (New Energy and Industrial Technology Development Organization in Japan).
Thanks are due to NEDO staffs, we were advised by about all of this development.

REFERENCES

(Book)
Wladimir Tiraspolsky and William C. Maurer, (1942-1982) *Hydraulic Downhole Drilling Motors* Editions technip, Paris. 562pp.

(Journal Article)
Volker Krueger, *Extended-length downhole mud motor designed for more power*. Oil & Gas Journal(Mar.25,1996) pp.70-75.

(Report)
Hikaru Kamiirisa and Tsuguhiko Watanabe (1998) *Trial manufactures and performance tests of the downholemotor with a trochoidal section.* Proceedings of 13th Symposium on Fluid Control, Tokyo, 1998. pp.41-44.

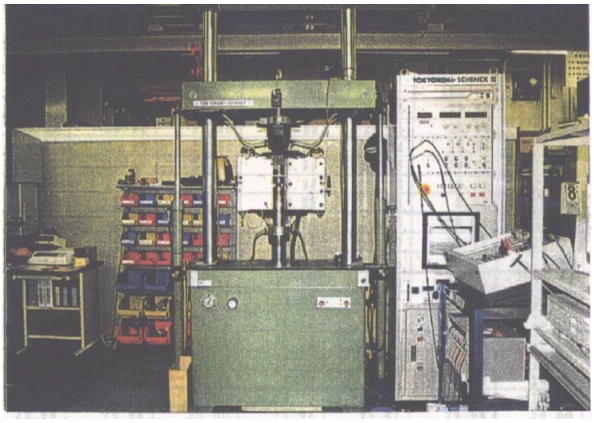

Fig. 1 Elastic recovery test equipment

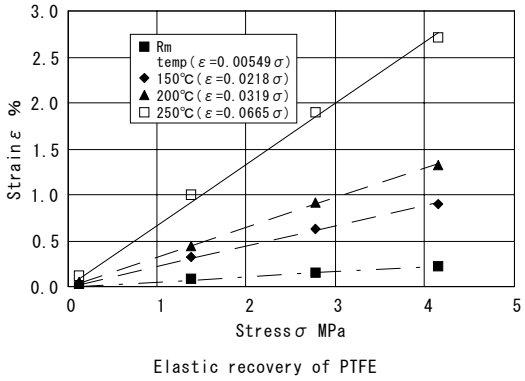

Fig.2 Elastic recovery of some elastomer

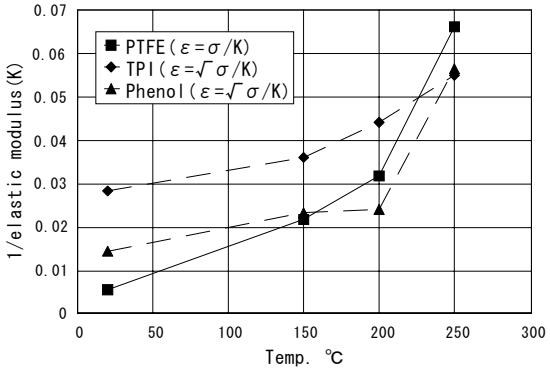

Fig.3 Alternation of elastic recoveries

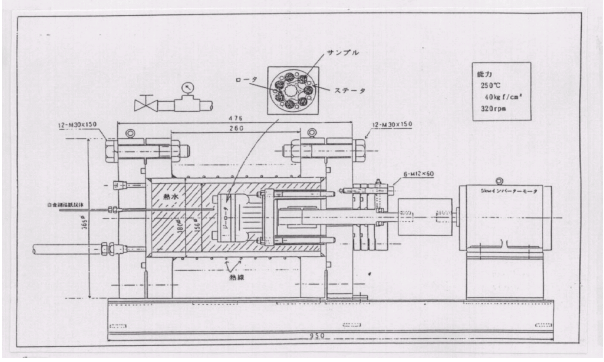

Fig.5 Abrasion test equipment

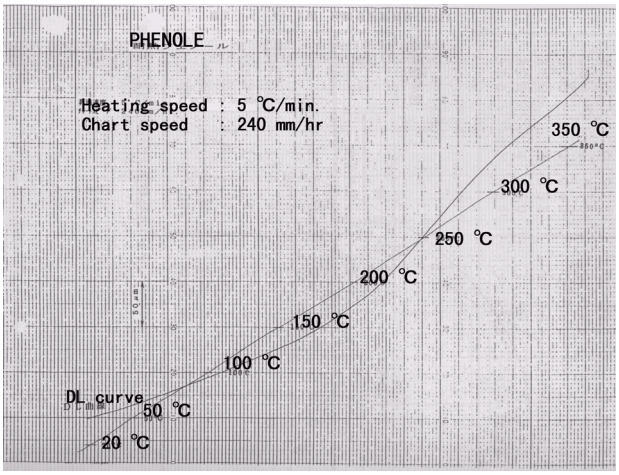

Fig.4 Thermal expansion

Fig.6 Results of abrasion tests
(Samples before the test (upper)
Samples after the test(lower))

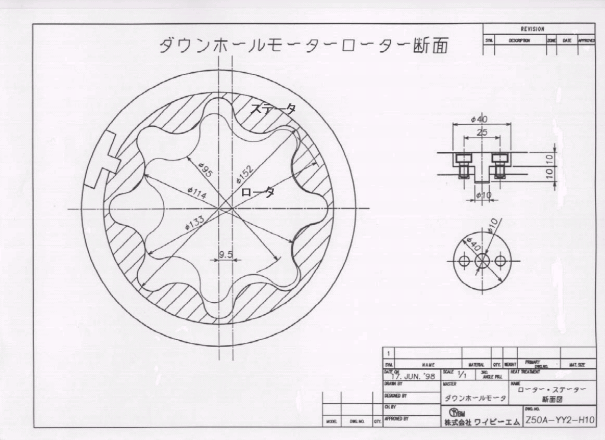

Fig.7 Section design

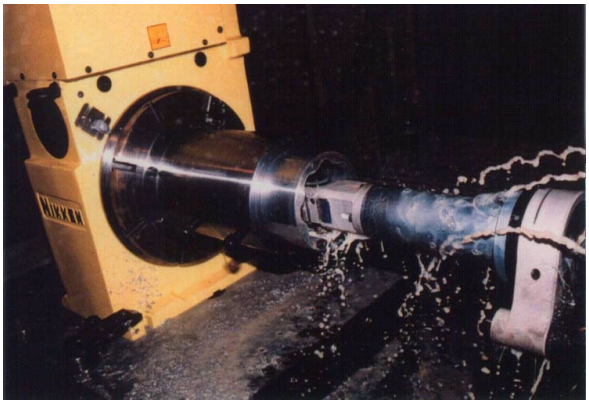

Fig.8 Numerical controlled machining center

Table.1 Designed parameters

			Rotor	Stator
Section parameters	Robes		7	8
	Base-circle diameters	mm	90.90	99.90
	Eccentricity	mm	9.5	9.5
	Off-set	mm	20.91	20.91
Adjustment	Clearance	mm	0.0	
Manufactured sizes	Diameters Maximum	mm	133.00	152.00
	Diameters Mininum	mm	95.00	114.00
	Total length	mm	583.33	291.67
	Twisted angle	deg	514.44	226.80
3-dimension parameters	Lead	mm	408.33	466.67
	Pitch	mm	58.33	58.33

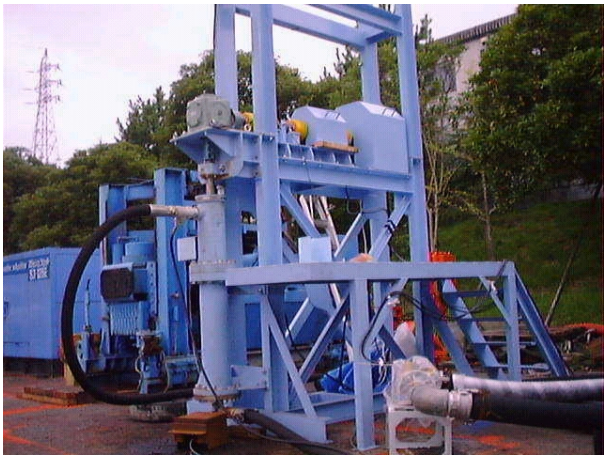

Fig.9 View of the experimental apparatus (Performance test)

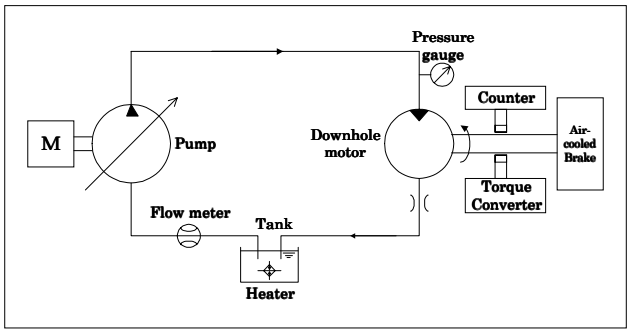

Fig.10 Arrangement of the experimental apparatus

Fig.11 Rotor and stator manufactured experimentally

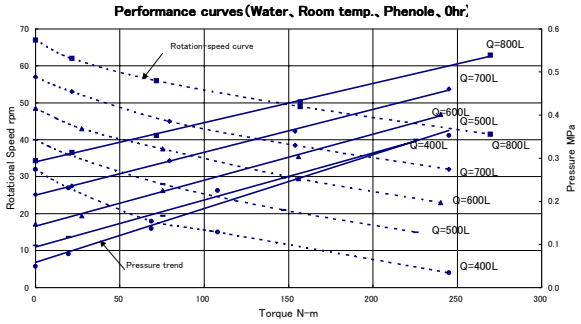

Fig.12 Performance curves @ Room temp. 0 hr

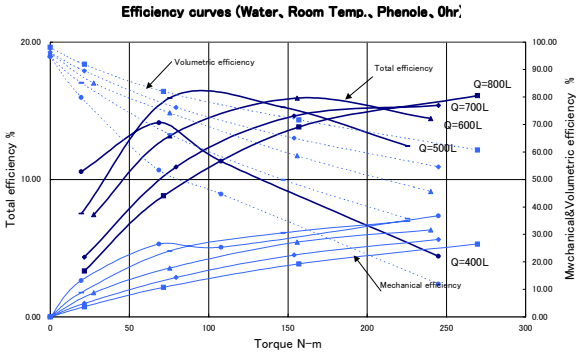

Fig.13 Efficiency curves @ Room temp. 0hr

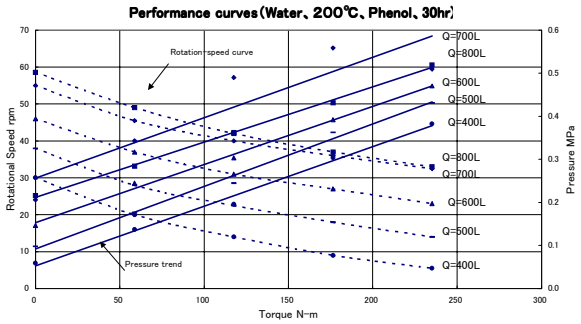

Fig.14 Performance curves @ 200℃ 30hr

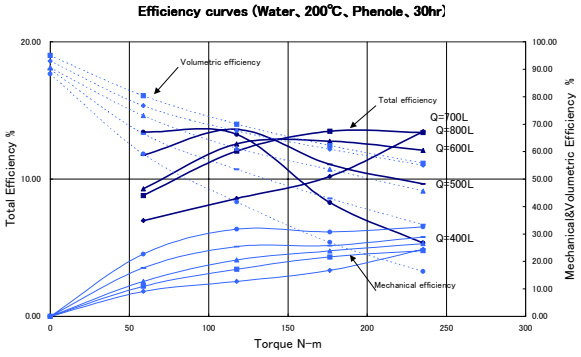

Fig.15 Efficiency curves @ 200℃ 30hr

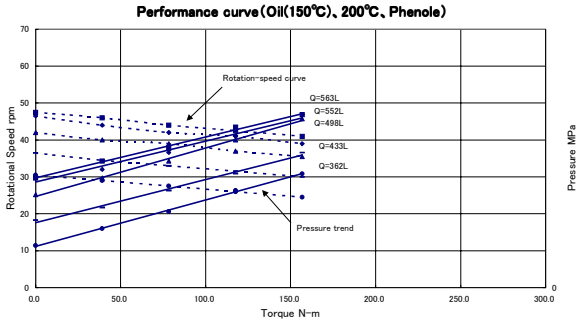

Fig.16 Performance curves @200℃ oil-circulation

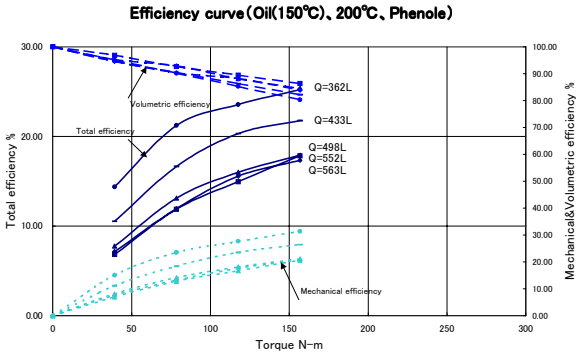

Fig.17 Efficiency curves @ 200℃ oil circulation

Table.2 Comparison with viscosities

	Water (JIS Z 8803)	Oil (applied to p.tests)	Drilling mud (BMP,SG=1.06)
Specfic gravity			
@ 15℃	1.0	0.9	
@ 150℃		0.8	
viscosityceefficient	cSt @1atm	cSt @1atm	
@ 20℃	1.0	2044	
@ 40℃	0.7	482	
@100℃	0.3	34	
@150℃		8.8	
Viscosity	10^3 × Pa·s	10^3 × Pa·s	10^3 × Pa·s
@ 20℃	1.0	1808	41 ～ 67
@ 40℃	0.7	420	28 ～ 48
@100℃	0.3	28	14 ～ 25
@150℃		7.0	7 ～ 12.5